Journal of Ceramic Processing Research. Vol. 25, No. 2, pp. 228~233 (2024)
(Received 6 January 2024, Received in revised form 27 March 2024, Accepted 28 March 2024)
https://doi.org/10.36410/jcpr.2024.25.2.228

J O U R N A L O F
Ceramic Processing Research

Effect of air flow rate on preparation of boron carbide by sol-gel low-temperature pyrolysis system

Chengcheng Tian[a,b,c], Yang Li[e], Yuanxia Wang[a,b,*], Ying Shi[a,d], and Li-Zhi Liu[a,b,c]
[a]*Polymer High Functional Film Engineering Research Center of Liaoning Province, Shenyang University of Chemical Technology, Shenyang, 110142, People's Republic of China*
[b]*School of Materials Science and Engineering, Shenyang University of Chemical Technology, Shenyang, 110142, People's Republic of China*
[c]*School of Materials Science and Engineering, Shenyang University of Technology, Shenyang, 110870, People's Republic of China*
[d]*Research and Development, Dongguan HAILI Chemical Material CO., LTD, Dongguan, 523808, People's Republic of China*
[e]*Alcohol Fuel Cell Research Group, Qingdao Institute of Bioenergy and Bioprocess Technology, Chinese Academy of Sciences, Qingdao, 266101, People's Republic of China*

The morphology and particle size of boron carbide in the sol-gel low-temperature pyrolysis system were controlled by changing the air flow rate during the pyrolysis of boric acid glycerin system. Analyzed the infrared absorption properties of condensation products and pyrolysis products, as well as the carbon network structure of pyrolysis products and the microstructure, phase composition, and particle size of boron carbide powder. The research results indicate that the air flowing in the pyrolysis atmosphere can accelerate the thermal decomposition efficiency of boric acid glycerol condensate and effectively reduce the pyrolysis temperature. The faster the air flow rate during the pyrolysis process, the denser the carbon network structure, smaller pore size, and more pores in the pyrolysis products, and the better the dispersion of boron oxide. In the boric acid glycerol system, with the increase of pyrolysis gas flow rate, the average particle size of boron carbide decreases from 10 μm to about 2 μm. In addition, the morphology of boron carbide changes from a hexagonal diamond to a smoother morphology. This indicates that by changing the air flow rate during the pyrolysis process, the carbon network structure of the pyrolysis products can be improved, thereby controlling the morphology and particle size of boron carbide. This paper provides a new method for the study of the sol-gel low-temperature pyrolysis method to accurately control the morphology of boron carbide.

Keywords: Boron carbide, Sol-gel Low-temperature pyrolysis, Pyrolysis air flow rate, Carbon mesh structure, Glycerol.

Introduction

Boron carbide is a highly refractory material with great application value in building structures and electronic processing [1-3]. It has many excellent properties, such as high temperature stability [4], high hardness [5], high electron capture cross-section, and excellent high-temperature thermoelectric performance [6]. The combination of these characteristics has brought many applications, such as being used as wear-resistant materials, ceramic armor, neutron moderators in nuclear reactors, and potential deep space flight power generation applications [7-10].

The preparation of boron carbide powder by sol-gel method is currently the best method to control the growth morphology and particle size of boron carbide at the molecular level [11, 12]. Boric acid serves as the boron source, while organic matter serves as the carbon source, such as glycerol [13-15], polyvinyl alcohol [16-19], sucrose [20], glucose [21], tartaric acid [22], cellulose [23], citric acid [24, 25], phenolic resin [26]. In the initial research, Hadian et al. [27] dehydrated and condensed boric acid and glucose at 180 °C to synthesize boric acid glucose gel. The gel was placed in a graphite boat and heated in a resistance furnace at about 1500-1600 °C for 1 h to generate boron carbide particles with micron crystal shape. However, the boron carbide prepared by this method has low purity and uneven particle size. Then Pilladi et al. [28] added the step of pyrolysis precursor by improving the method of sol-gel. The dry gel of boric acid and sucrose is heated at about 600 °C in the air to carbonize the organic matter in the dry gel, and boric acid is converted into boron oxide. The pyrolysis products were subjected to a carbon thermal reduction reaction to prepare boron carbide powder with a residual carbon content of about 3%, uniform particle size, and high purity. The successful preparation of boron carbide powder with high purity, small particle

*Corresponding author:
Tel : 13504946630
E-mail: wangyuanxia@aliyun.com

size, and uniform morphology has been a hot topic for researchers in this field [29-31]. Therefore, Kakiage et al. [14] further refined the steps of pyrolysis precursors. Preliminary pre pyrolysis is carried out in the early stage of pyrolysis, that is, the sol-gel is pyrolyzed at 250 °C for 2 h, heated continuously to 350 °C for 2 h, and finally completely pyrolyzed at 450-650 °C. By improving the method of pyrolysis precursors, the controllability of preparing boron carbide was enhanced, and more uniform morphology and particle size of boron carbide powder were obtained. Researchers have conducted extensive research on the dose of raw materials used in the preparation of boron carbide, as well as the time and temperature of pyrolysis and carbothermal reduction reactions [32-36]. In the research, most of the pyrolysis precursors were completed in air, and there was no in-depth study on the effect of different rates of air as the pyrolysis atmosphere on boron carbide.

In this study, boric acid was used as the boron source and glycerol as the carbon source. On the basis of previous studies, boron carbide powder was prepared by carbothermal reduction reaction using the sol-gel pyrolysis precursor method. The main focus of this study is the influence of air flow rate in the pyrolysis atmosphere on the morphology and particle size of boron carbide powder. This part of the research will further enhance the low-temperature pyrolysis preparation technology of boron carbide.

Experiment

Materials

Boric acid (BA) (99.9%) purchased from Bor Mining Chemical Company, Russia. Glycerin (Gl) (99.0%) purchased from Sinopharm Chemical Reagent Co., Ltd, Shanghai, China. These materials were used as received without any prior treatment in this work.

Experimental methods

Mix equimolar amounts of boric acid and glycerol, and then dehydrate at 150 °C to prepare a condensed product, which is a transparent glassy solid. Place the condensed product in an alumina crucible and heat it in air at 250 °C for 2 hours, then heat it in air at 350 °C for 2 hours, and then pyrolysis condensed product in air at 450 °C, 500 °C, 550 °C, 600 °C, 650 °C or 700 °C for 2 hours to obtain the pyrolysis product that removes excess carbon. The pyrolysis air flow rates are 100 ml/min, 200 ml/min, and 300 ml/min respectively (to compare with previous studies on pyrolysis air flow rates of 0 ml/min [14]), and the above steps are continuously carried out using a temperature programmed muffle furnace. After grinding in an agate mortar, the obtained black pyrolysis product powder was placed in a graphite boat and subjected to a carbon thermal reduction reaction at 1450 °C for 2 hours to prepare boron carbide powder.

Analysis methods

The infrared spectra of condensation products and pyrolysis products were measured using the Shimadzu IRPrestige-21 spectrometer. Measurement using transmission method of KBr particles and monochromatic CuK_α Radiation powder X-ray diffractometer (Rigaku RAD-C) was used to analyze the phase of the product by X-ray diffraction (XRD); estimate the crystallization behavior of boron carbide based on the peak intensity ratio of B_4C [$I_{B4C}/(I_{B4C}+IC+I_{B2O3})$], where boron carbide [$I_{B4C}$] is 2θ=37.8°, free carbon [IC] is 2θ=26°, boron oxide [I_{B2O3}] is 2θ=27.8°; use Hitachi SU8010 field emission scanning electron microscope (FE-SEM) to scan and analyze the microstructure of boron carbide powder and pyrolysis product carbon mesh structure at 15.0 kV; the pyrolysis product powder is washed with hot water to recover the B_2O_3 component (adding mannitol to form the mannitol H_3BO_3 complex), and the remaining residue is weighed as carbon content. Using phenolphthalein as an indicator, titrate the mannitol-H_3BO_3 complex with sodium hydroxide solution, determine the content of B_2O_3 in the pyrolysis product powder, and determine the ratio of C/B_2O_3 in the pyrolysis product; the particle size of boron carbide products was determined by the Marvin 3000 laser particle size analyzer.

Results and Discussion

The effect of air flow rate on the thermal decomposition efficiency of condensation products

Figure 1 shows the infrared analysis spectra of boric acid-glycerol condensate and pyrolysis products at 500 °C. In Fig. 1a, the C-O absorption stretching vibration peak at 1041 cm^{-1} and the B-OH bending vibration peak at 1288 cm^{-1} are characteristic peaks of the condensation product. However, it has disappeared in Figs. 1(b-e),

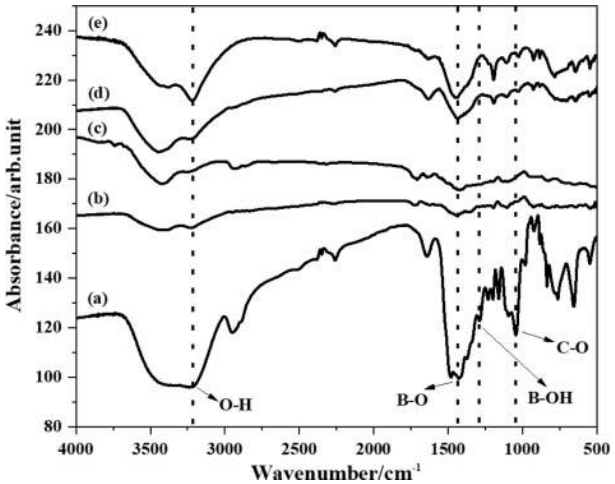

Fig. 1. Infrared spectra of boric acid-glycerol condensate (a) and the pyrolysis products of different pyrolysis air flow rates, pyrolyzed at 500 °C for 2 h, the pyrolysis air flow rates are (b) 0 ml/min, (c) 100 ml/min, (d) 200 ml/min and (e) 300 ml/min, respectively.

indicating that the 500 °C condensate has completely pyrolyzed and transformed into a mixture of boron oxide and amorphous carbon [37]. In Fig. 1(b-e), the absorption band exhibits B-O stretching vibration peak near 1450 cm^{-1}. As the pyrolysis atmosphere flow rate increases, the B-O binding strength gradually increases. This is due to the acceleration of the pyrolysis atmosphere flow rate, which increases the reaction rate of the pyrolysis system. The possible reason is that the flow rate of the pyrolysis atmosphere can accelerate the efficiency of the thermal decomposition of the condensate. The higher the air flow rate, the higher the oxygen content, which accelerates the carbonization rate of the entire system.

The effect of air flow rate on the carbon boron ratio of pyrolysis products

Generally speaking, the carbon thermal reduction complete reaction is very difficult because the byproducts of the reaction (such as CO) take volatile borides away from the reaction site, which breaks the stoichiometric equilibrium [38]. In order to determine the optimal carbon content of the pyrolysis product of boric acid-glycerol, the weight ratio of B_2O_3 and remaining carbon in the pyrolysis product was removed with hot water to calculate the molar ratio of carbon to boron oxide. According to the chemical reaction equation (1), the stoichiometric ratio C/B_2O_3 molar ratio of the reaction can be calculated to be 3.5.

$$2\ B_2O_3+7\ C=B_4C+6\ CO \quad (1)$$

Previous researchers have controlled the C/B_2O_3 molar ratio by adjusting the pyrolysis temperature, and believed that volatile boron oxides were formed during the carbon thermal reduction process above 1050 °C, leading to the volatilization of B_2O_3 and a decrease in boron content in the system [6]. Therefore, the molar ratio of C/B_2O_3 is controlled at around 3.5 to synthesize boron carbide powder with minimal carbon residue. In addition, the carbon thermal reduction system contains dispersed B_2O_3 particles, and the C/B_2O_3 molar ratio will continue to be adjusted to suppress residual carbon in boron carbide powder [39].

Figure 2 shows the C/B_2O_3 ratio variation spectrum of the pyrolysis products obtained from the condensation products of boric acid and glycerol under different air flow rates in pyrolysis atmospheres. When the pyrolysis temperature is 500 °C, the ratio of pyrolysis product C/B_2O_3 decreases with the increase of pyrolysis gas flow rate. This is due to the fast airflow speed and high oxygen content, which can carry or oxidize a portion of the carbon source through the airflow. This accelerates the reaction process and promotes the stoichiometric ratio of C/B_2O_3 to approach a reasonable range. Moreover, some researchers [40] have pointed out that it is difficult to strictly control the composition of pyrolysis products by controlling the thermal decomposition temperature,

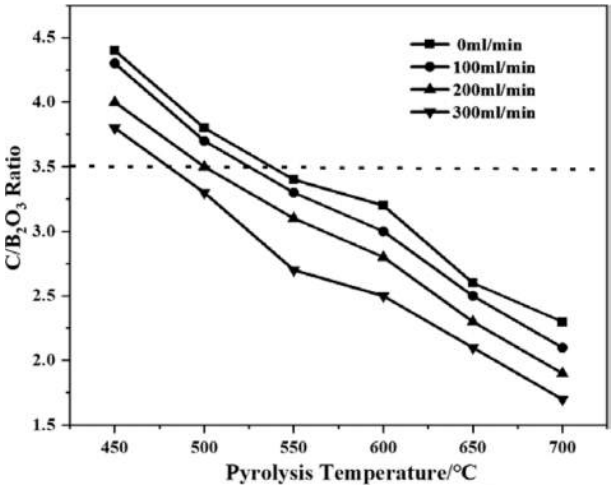

Fig. 2. Change in C/B_2O_3 ratio of pyrolysis products of boric acid-glycerol condensate pyrolysis at 450-700 °C for 2 h with air flow rates of 0 ml/min, 100 ml/min, 200 ml/min and 300 ml/min respectively.

as too high a pyrolysis temperature can promote the fracture of polymer chains. So, by controlling the gas flow rate, the problem of polymer chain breakage can be effectively solved.

Microscopic analysis of carbon mesh from pyrolysis products

Figure 3 shows the thermal decomposition product of boric acid glycerol condensate after 2 h of heat treatment at 500 °C, followed by carbon mesh structure after hot water washing. The results shown in Fig. 3a indicate that when the air flow rate is 0 ml/min, the pore size of the carbon mesh is approximately 2-3 um, and the size of

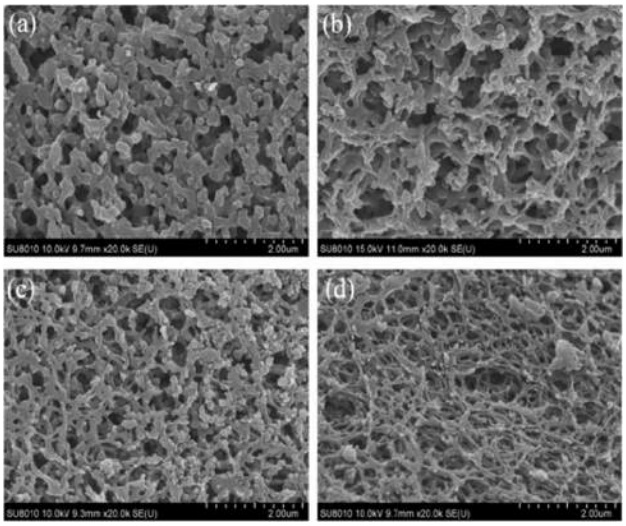

Fig. 3. SEM of carbon net structure of the pyrolysis products of boric acid-glycerol condensate pyrolysis at 500 °C for 2 h in different pyrolysis air flow rates after removal of B_2O_3 by washing in hot water, the pyrolysis air flow rates are (a) 0 ml/min, (b) 100 ml/min, (c) 200 ml/min and (d) 300 ml/min, respectively.

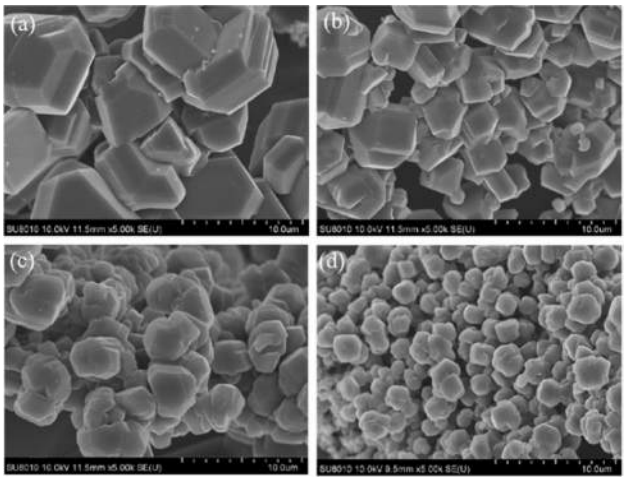

Fig. 4. SEM of the microstructure of boron carbide formed by the pyrolysis product of boric acid-glycerol condensate pyrolysis at 500 ℃ for 2 h at different pyrolysis air flow rates and carbothermal reduction at 1450 ℃ for 2 h, the pyrolysis air flow rates are (a) 0 ml/min, (b) 100 ml/min, (c) 200 ml/min and (d) 300 ml/min, respectively.

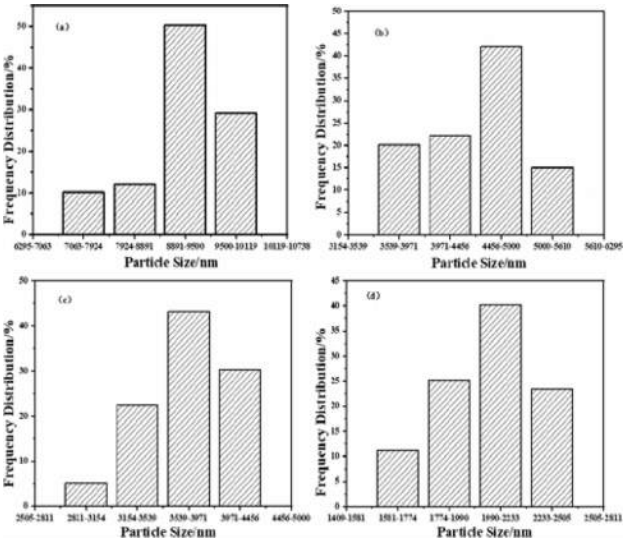

Fig. 5. Particle size analysis diagram of boron carbide formed by the pyrolysis product of boric acid-glycerol condensate pyrolysis at 500 ℃ for 2 h at different pyrolysis air flow rates and carbothermal reduction at 1450 ℃ for 2 h, the pyrolysis air flow rates are (a) 0 ml/min, (b) 100 ml/min, (c) 200 ml/min and (d) 300 ml/min, respectively.

the carbon mesh skeleton is around 2 um. When the air flow rate is 100 ml/min, the pore size of the carbon mesh significantly decreases to below 2 um, and the lines of the carbon mesh skeleton also become significantly thinner (Fig. 3b). When the flow rate of pyrolysis gas reaches 300 ml/min, the carbon web structure becomes more uniform, similar to a spider web structure (Fig. 3d). By accelerating the flow rate of pyrolysis gas, the carbon mesh structure can become more and more orderly, the pore size of the carbon mesh is gradually decreasing, and the lines of the carbon mesh skeleton are also gradually becoming thinner. Therefore, the acceleration of pyrolysis gas flow rate helps to densify the carbon network structure and does not damage the carbon skeleton of organic matter.

Microscopic morphology and particle size analysis of boron carbide

Figure 4 shows the microstructure of boron carbide produced by the pyrolysis of boric acid glycerol condensate at 500 ℃ for 2 hours, with pyrolysis air flow rates of (a) 0 ml/min, (b) 100 ml/min, (c) 200 ml/min, and (d) 300 ml/min, respectively, after being reduced by carbothermal reduction at 1450 ℃ for 2 hours. Comparing the morphology of boron carbide particles in Figs. 4(a-d) with the morphology of carbon mesh in Figs. 3(a-d), the particle size of boron carbide in Fig. 4a exhibits sharp rhombic crystals, which may be related to the loosely connected carbon mesh, slightly coarse carbon skeleton, and large pore size in Fig. 3a. The morphology of boron carbide in Figs. 4(b-d) tends to be more rounded from sharp diamond angles, which may be related to the increasingly compact carbon network structure in Figs. 3(b-d). The average particle size of boron carbide (as shown in Figs. 4(a-d) and 5(a-d)) gradually decreases from around 10 μm to 2 μm, which may be related to the acceleration of pyrolysis airflow, resulting in a decrease in the carbon mesh size of pyrolysis products. On the other hand, due to the carbon mesh structure in the pyrolysis products acting as a carbon template, it affects the morphology of boron carbide. The denser the carbon mesh structure, the smaller the pore size of the carbon mesh, resulting in an increase in the number of carbon mesh pores, and an increase in the nucleation sites of boron oxide and carbon. Therefore, a high flow rate and low-temperature pyrolysis atmosphere have a positive effect on the preparation of boron carbide with small particle size and good dispersion.

Phase analysis of boron carbide

Figure 6 shows the phase analysis of boron carbide prepared by the carbothermal reduction reaction in the boric acid glycerol system. From Fig. 6, it can be seen that the characteristic diffraction peak of boron carbide (2θ=20.08°, 22.34°, 23.89°, 32.31°, 35.29°, 38.12°), and it can also be seen from Fig. 6ab that the diffraction peak intensity of free carbon is relatively high (2θ= 26.25°). Based on the analysis in section 3.2, it can be concluded that when the air flow rates in the pyrolysis products at 500 ℃ are 0 ml/min and 100 ml/min, the C/B_2O_3 ratios are 3.8 and 3.7, respectively, exceeding the optimal stoichiometric ratio. This is an important reason for the presence of free carbon in boron carbide. There are very small particles attached to the boron carbide particles in Figs. 4a and 4b, which may be small free carbon powders. In Figs. 6c and 6d, the diffraction peaks of free carbon are not obvious. This is due to the introduction

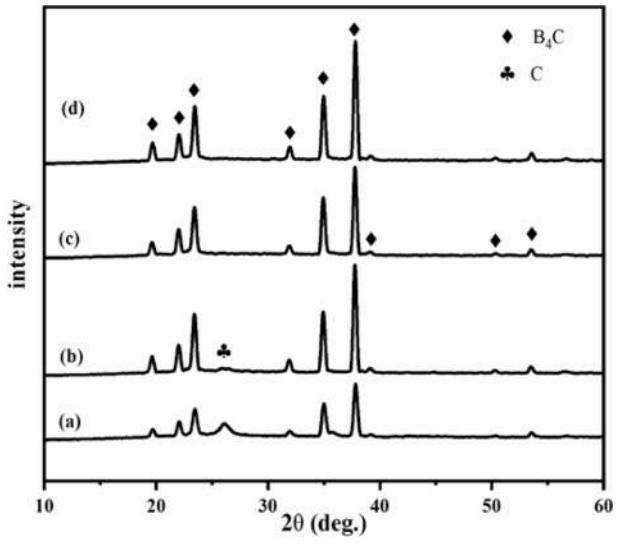

Fig. 6. XRD patterns of boron carbide formed by the pyrolysis product of boric acid-glycerol condensate pyrolysis at 500 ℃ for 2 h at different pyrolysis air flow rates and carbothermal reduction at 1450 ℃ for 2 h, the pyrolysis air flow rates are (a) 0 ml/min, (b) 100 ml/min, (c) 200 ml/min and (d) 300 ml/min, respectively.

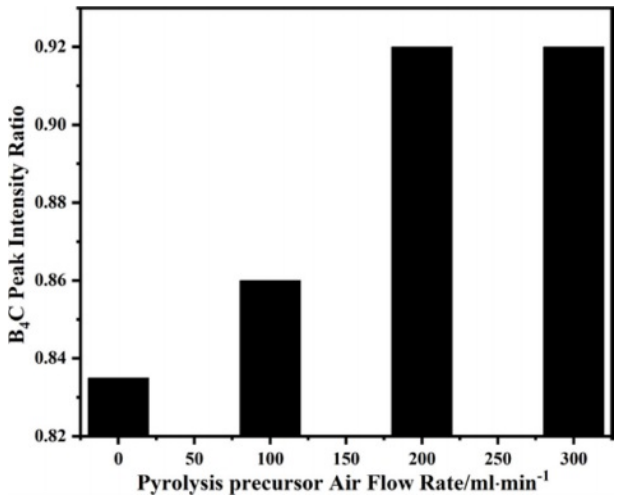

Fig. 7. Pyrolysis products of boric acid-glycerol condensate at 500 ℃ for 2 h with pyrolysis air flow rates of 0-300 ml/min. Changes in B_4C peak intensity ratio of different pyrolysis products after carbothermal reduction at 1450 ℃ for 2 h.

of pyrolysis atmosphere, which causes the ratio of C/B_2O_3 to be close to or lower than the stoichiometric ratio of 3.5, resulting in the formation of boron carbide containing very small amounts of impurities. This result also indicates that introducing air during the pyrolysis process can effectively reduce the pyrolysis temperature.

Based on the XRD results in Figs. 6(a-d), plot the peak intensity ratio curves of boron carbide prepared from pyrolysis products at different flow rates (as shown in Fig. 7). From Fig. 7, it can be seen that with the increase of pyrolysis air flow rate, the peak intensity ratio of B_4C increases rapidly, indicating that the crystallization behavior of boron carbide is becoming more and more perfect [41]. The pyrolysis product with an air flow rate of 200 ml/min corresponds to less free carbon in boron carbide powder. The boron carbide powder corresponding to the pyrolysis product with an air flow rate of 0 ml/min contains a significant amount of free carbon, which also indicates that the purity of boron carbide is positively correlated with the gas flow rate during the pyrolysis process in the same pyrolysis treatment environment and carbon thermal reduction process. It is worth noting that the peak intensity ratio of boron carbide corresponding to 300 ml/min pyrolysis product to that corresponding to 200 ml/min pyrolysis product remains almost unchanged (Fig. 7). At this point, the content of free carbon in the two types of boron carbide is almost the same, which means that the structure of uniformly arranged pyrolysis products can achieve uniform dispersion of reactants by controlling reaction conditions. The arrangement of boric acid glycerol after pyrolysis is similar to that of block copolymers in porous materials, which is an ideal self-assembled organic material for preparing boron carbide [42]. This means that the precise structure of pyrolysis products can be achieved through low-temperature heat treatment and the combination of pyrolysis gas flow rate.

Conclusion

On the basis of summarizing the previous experiments, the influence of the air flow rate during pyrolysis on the preparation of boron carbide in the sol-gel low-temperature pyrolysis system was investigated. The faster the air flow rate during the pyrolysis process, the higher the content of boron oxide in the pyrolysis product of boric acid glycerol condensate. The faster decomposition of condensed matter in the pyrolysis system leads to a significant improvement in pyrolysis efficiency. The rapid pyrolysis airflow leads to a faster decrease in the ratio of C/B_2O_3 in the pyrolysis products, effectively reducing the pyrolysis temperature of the pyrolysis reaction system. More importantly, the rapid air flow rate causes the carbon mesh structure in the pyrolysis products to develop towards higher density, smaller pore size, and more pores. On the one hand, it enhances the dispersion of boron oxide in the carbon network, increases the nucleation sites of boron oxide, and helps to shorten the process of carbon thermal reduction reaction. On the other hand, by precisely controlling the air flow rate during the pyrolysis process, the particle morphology and size of boron carbide powder can be effectively controlled.

Acknowledgement

The authors would like to acknowledge financial support from Key Laboratory of Liaoning Province for Polymer Catalytic Synthesis, Liaoning Provincial Engineering

Laboratory for Advanced Polymeric Materials and High-tech Research and Development Project of Liaoning Provincial Industrial Special Resources Protection Office (Liao Cai Qi [2013] 736).

References

1. H.Z. Li, H.K. Wei, H.J. Qiu, Y.K. Wang, C.A. Wang, and Z.P. Xie, J. Ceram. Process. Res. 24[1] (2023) 1-7.
2. Y. Li, S.X. Li, W. Song, C.C. Tian, and O.T. Ayode, J. Ceram. Process. Res. 24[2] (2023) 367-373.
3. C.A. Sun, X.G. Lu, Y.B. Chen, L.L. Zuo, and Y.K. Lie, J. Ceram. Process. Res. 22[3] (2021) 340-344.
4. Q.L. Li, Y. Yang, Y.Q. Wei, M. Liu, H.J. Zhou, T.L. Huo, and Z.R. Huang, Mater. Rep. 35[2] (2021) 2006-2011.
5. P. Svec, Z. Gabrisova, and A. Brusilova, J. Ceram. Process. Res. 20[1] (2019) 113-120.
6. Y. Li, S.X. Li, S. Wang, C.C. Tian, and T.A. Otitoju, J. Ceram. Process. Res. 23[5] (2022) 595-610.
7. R. Adeli, S.P. Shirmardi, and S.J. Ahmadi, Radiat. Phys. Chem. 127 (2016) 140-146.
8. K.M. Senthilkumar, A. Sivakumar, R.M. Shivaji, S.K. Tamang, and M. Giriraj, J. Ceram. Process. Res. 23[2] (2022) 233-236.
9. J. Kenny, N. McDonald, J. Binner, I.T.H. Chang, and S. Marinel, J. Eur. Ceram. Soc. 42[2] (2022) 383-391.
10. P.H. Li, M.D. Ma, Y.J. Wu, X. Zhang, Y.K. Chang, Z.W. Zhuge, L. Sun, W.T. Hu, D.L. Yu, B. Xu, Z.S. Zhao, J.Y. Chen, J.L. He, and Y.J. Tian, J. Eur. Ceram. Soc. 41[7] (2021) 3929-3936.
11. O. Karaahmet, and B. Cicek, Ceram. Int. 48[9] (2022) 11940-11952.
12. S. Avcioglu, F. Kaya, and C.C. Kaya, Ceram. Int. 47[19] (2021) 26651-26667.
13. S.K. Vijay, R. Krishnaprabhu, V. Chandramouli, and S. Anthonysamy, Ceram. Int. 44[5] (2018) 4676-4684.
14. M. Kakiage, N. Tahara, I. Yanase, and H. Kobayashi, Mater. Lett. 65[12] (2011) 1839-1841.
15. M. Kakiage, and T. Kobayashi, Mater. Lett. 254 (2019) 158-161.
16. N. Shawgi, S.X. Li, and S. Wang, Ceram. Int. 43[13] (2017) 10554-10558.
17. N. Shawgi, S.X. Li, S. Wang, Y. Li, and R. Ramzi, Ceram. Int. 44[1] (2018) 774-778.
18. N. Shawgi, S.X. Li, S. Wang, Y. Li, and R. Ramzi, Ceram. Int. 44[8] (2018) 9887-9892.
19. M. Kakiage, N. Tahara, S. Yanagidani, I. Yanase, and H. Kobayashi, J. Ceram. Soc. Jpn. 119[1390] (2011) 422-425.
20. J.L. Watts, P.C. Talbot, J.A. Alarco, and I.D.R. Mackinnon, Ceram. Int. 43[2] (2017) 2650-2657.
21. D. Kozien, P. Jelen, M. Sitarz, and M.M. Bucko, Int. J. Refract. Met. H. 86 (2020) 105099.
22. N. Tahara, M. Kakiage, I. Yanase, and H. Kobayashi, J. Alloy. Compd. 573 (2013) 58-64.
23. Y.C. Zheng, Z.Q. Lia, J. Xu, T.L. Wang, X. Liu, X.H. Duan, Y.J. Ma, Y. Zhou, and C.H. Pei, Nano Energy 20 (2016) 94-107.
24. A. Sinha, T. Mahata, and B.P. Sharma, J. Nucl. Mater. 301[2-3] (2002) 165-169.
25. A.K. Khanra, B. Mater. Sci. 30[2] (2007) 93-96.
26. A. Najafi, F. Golestani-Fard, H.R. Rezaie, and N. Ehsani, J. Alloy. Compd. 509[37] (2011) 9164-9170.
27. A.M. Hadian, and J.A. Bigdeloo, J. Mater. Eng. Perform. 17[1] (2008) 44-49.
28. T.R. Pilladi, K. Ananthasivan, S. Anthonysamy, and V. Ganesan, J. Mater. Sci. 47[4] (2012) 1710-1718.
29. P. Asgarian, A. Nourbakhsh, P. Amin, R. Ebrahimi-Kahrizsangi, and K.J.D. MacKenzie, Ceram. Int. 40[10] (2014) 16399-16408.
30. F. Farzaneh, F. Golestanifard, M.S. Sheikhaleslami, and A.A. Nourbakhsh, Ceram. Int. 41[10] (2015) 13658-13662.
31. E. Karacay, E. Alp, and H.C. Cabbar, J. Fac. Eng. Archit. Gaz. 27[2] (2012) 417-428.
32. Y.J. Liu, Q. Tian, S.Q. Wang, Z.Q. Li, X.H. Duan, L.K. Que, and C.H. Pei, Ceram. Int. 46[11] (2020) 18131-18141.
33. Y. Li, S.X. Li, S. Wang, and C.C. Tian, J. Ceram. Process. Res. 24[1] (2023) 134-141.
34. O. Karaahmet, and B. Cicek, Ceram. Silikaty 64[4] (2020) 434-446.
35. N. Shawgi, S.X. Li, S. Wang, Z. Wang, and Y.N. Nie, J. Sol.-Gel. Sci. Techn. 82[2] (2017) 450-457.
36. S. Mondal and A. K. Banthia, J. Eur. Ceram. Soc. 25[2-3] (2005) 287-291.
37. R. Ramzi, S. Wang, N. Shawgi, S.X. Li, and T. Tang, Mater. Res. Express. 6[3] (2018) 539-549.
38. T.R. Pilladi, K. Ananthansivan, and S. Anthonysamy, Powder Technol. 246 (2013) 247-251.
39. L.H. Bao, C. Li, Y. Tian, J.F. Tian, C. Hui, X.J. Wang, C.M. Shen, and H.J. Gao, Chinese Phys. B 17[12] (2008) 4585-4591.
40. B. Ozcelik and C. Ergun, J. Mater. Res. 31[18] (2016) 2789-2803.
41. H.V. SarithaDevi, M.S. Swapna, and S. Sankararaman, J. Mater. Sci.-Mater. El. 32[6] (2021) 7391-7398.
42. M. Kakiage, J. Ceram. Soc. Jpn. 126[8] (2018) 602-608.